Table 4 Clinical and genetic parameters affecting PFS and OS in grade III gliomas with mutated *IDH1/2*

Characteristic	PFS				OS			
	No. (%)	5-year survival (%)	Median months	*P* (log-rank)	No. (%)	5-year survival (%)	Median months	*P* (log-rank)
	76	70.5	NR		76	82.3	NR	
Histology								
AA	35 (46)	71.8	NR	0.86 (vs AOA, AO)	35 (46)	82.6	NR	0.86 (vs AOA, AO)
AO	20 (26)	75.2	NR		20 (26)	89.2	NR	
AOA	21 (28)	64.4	NR		21 (28)	76.0	NR	
Age at diagnosis								
<50 years old	49 (64)	74.0	NR	0.20	49 (64)	81.0	NR	0.39
≥50 years old	27 (36)	61.4	68		27 (36)	85.7	87	
Sex								
Female	34 (45)	72.9	NR	0.29	34 (45)	92.6	NR	0.074
Male	42 (55)	68.7	NR		42 (55)	73.8	NR	
Karnofsky performance status								
≥80	62 (82)	69.2	NR	0.99	62 (82)	80.5	NR	0.45
<80	14 (18)	76.9	62		14 (18)	92.3	87	
Gross total resection								
Yes	30 (39)	80.5	NR	**0.040**	30 (39)	88.4	NR	**0.018**
No	46 (61)	63.0	74		46 (61)	78.5	NR	
Ki-67 labeling index								
<15%	27 (48)	81.7	NR	0.055	27 (48)	90.9	NR	0.15
≥15%	29 (52)	47.1	62		29 (52)	73.9	NR	
TP53								
Wild-type	40 (53)	80.8	NR	0.053	40 (53)	90.2	NR	**0.046**
Mutated	36 (47)	59.3	NR		36 (47)	73.1	NR	
1p/19q codeletion								
Yes	30 (39)	74.3	NR	0.69	30 (39)	87.4	NR	0.48
No	46 (61)	68.1	NR		46 (61)	78.9	NR	
Gain of 7p								
No	68 (89)	73.4	NR	0.089	68 (89)	86.4	NR	**0.017**
Yes	8 (11)	31.3	43		8 (11)	26.7	51	
Homozygous deletion of 9p								
No	73 (96)	71.4	NR	0.93	73 (96)	81.6	NR	0.67
Yes	3 (4)	50.0	77		3 (4)	100	82	
Loss of 10q								
No	70 (92)	71.8	NR	0.70	70 (92)	82.4	NR	0.97
Yes	6 (8)	55.6	NR		6 (8)	83.3	NR	
MGMT								
Methylated	69 (91)	70.2	NR	0.64	69 (91)	81.0	NR	0.82
Unmethylated	7 (9.0)	75.0	74		7 (9.0)	100	88	

AA anaplastic astrocytoma, *AO* anaplastic oligodendroglioma, *AOA* anaplastic oligoastrocytoma, *NR* not reached, *OS* overall survival, *PFS* progression-free survival

Bold indicates statistical significance at $P < 0.050$

multivariate analysis (Table 5). In the wild-type *IDH1/2* group, *TP53* gene status did not affect prognosis (Table 6).

EGFR alterations are frequently observed in grade III and IV gliomas, but the prognostic value is still controversial [23, 25–27]. In our series, 7p gain (*EGFR*

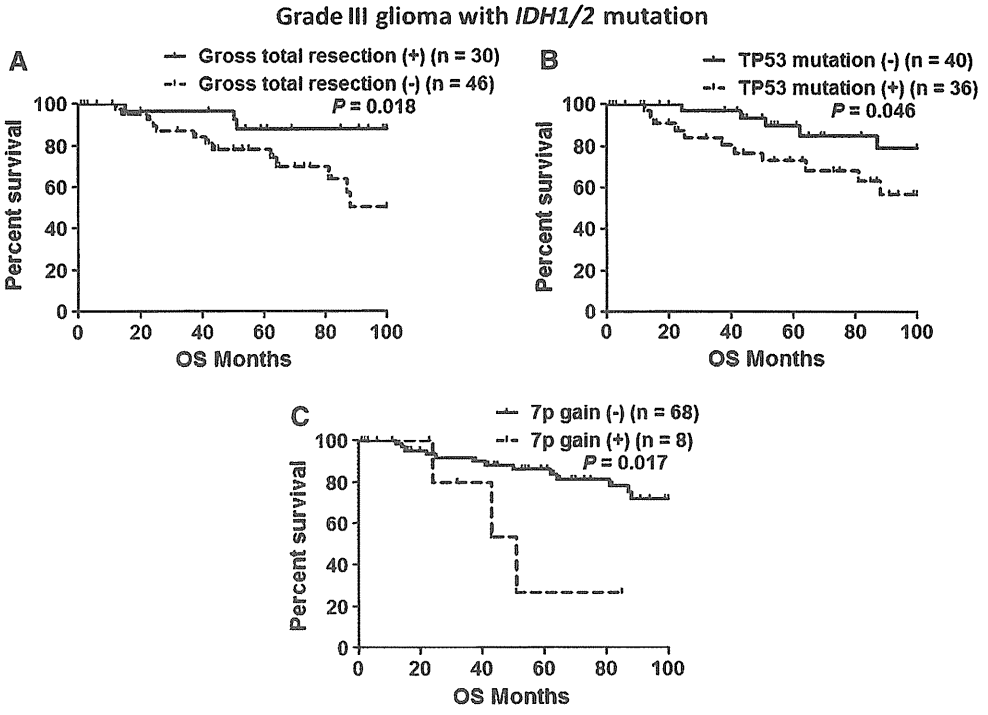

Fig. 2 Overall survival of patients with *IDH1/2*-mutated grade III gliomas by clinical and molecular markers. **a** Patients with gross total resection presented prolonged survival compared with patients with incomplete resection. **b** Patients with *TP53* mutation presented shorter survival compared with patients without *TP53* mutation. **c** Patients with 7p gain presented shorter survival compared with patients without 7p gain

Table 5 Multivariate analysis of independent factors associated with survival in grade III glioma patients with mutated *IDH1/2*

Variable	PFS			OS		
	Hazard ratio	95% CI	*P*	Hazard ratio	95% CI	*P*
Gross total resection						
Yes vs No			0.27	5.7	1.53–20.8	**0.0092**
7p (*EGFR*)						
Gained vs retained	5.3	1.35–20.5	**0.017**	5.5	1.39–21.5	**0.015**
TP53						
Mutated vs wild-type			0.15	3.4	1.15–9.8	**0.026**
Ki-67 labeling index						
≥15 vs <15%	3.2	1.11–9.05	**0.030**	N/A	N/A	N/A

OS overall survival, *CI* confidence interval, *N/A* not applicable

Bold indicates statistical significance at $P < 0.050$

amplification) was significantly associated with poor survival (Tables 2, 3). Furthermore, from the subgroup analysis, 7p gain was an independent prognostic factor of poor outcome in the mutated *IDH1/2* group (Tables 4, 5), but not in the wild-type *IDH1/2* group (Table 6). The frequency of 7p gain in grade III gliomas in the mutated *IDH1/2* group was small at 11% (Table 4), ranging from 0 to 43% in other reports [1, 3, 7]. Even in the mutated *IDH1/2* group, patients with *EGFR* amplification present poor prognosis, and careful follow-up is needed.

Including our data, 17–41% of grade III glioma patients had wild-type *IDH1/2* [1, 3, 8, 28]. The wild-type *IDH1/2* group consisted of 21 AA, 7 AOA, and 11AO. To exclude the possibility of diagnostic error in the present study, histology was re-reviewed by two neuropathologists. Surprisingly, neither necrosis nor microvascular proliferation was detected in this group, and therefore the wild-type *IDH1/2* group were histologically distinct from glioblastoma. In terms of prognosis, the median OS of patients with grade III gliomas with wild-type *IDH1/2* was 26 months, much shorter than the median OS of patients with grade III glioma with mutated *IDH1/2* (median not reached) (Tables 2, 4, 6), but longer than that of patients with primary glioblastoma (12.5–17 months) [13, 29]. In terms of genetic alterations, grade III gliomas with wild-type *IDH1/2* had only 10% of 10q alteration, 15% of homozygous

Table 6 Clinical and genetic parameters affecting PFS and OS in grade III glioma with wild-type *IDH1/2* group

Characteristic	PFS				OS			
	No. (%)	5-year survival (%)	Median months	*P* (log-rank)	No. (%)	5-year survival (%)	Median months	*P* (log-rank)
	39	13.5	13		39	26.3	26	
Histology								
AA	21 (54)	9.5	11	0.15 (vs AOA, AO)	21 (54)	18.2	18	0.094 (vs AOA, AO)
AO	11 (28)	0	18		11 (28)	46.7	40	
AOA	7 (18)	38.1	25		7 (18)	34.3	43	
Age at diagnosis								
<50 years old	18 (46)	15.7	13	0.71	18 (46)	23.2	18	0.25
≥50 years old	21 (54)	5.9	11		21 (54)	27.5	34	
Sex								
Female	11 (28)	18.2	11	0.60	11 (28)	39.8	43	0.36
Male	28 (72)	5.6	13		28 (72)	18.6	22	
Karnofsky performance status								
≥80	29 (74)	9.9	13	0.48	29 (74)	27.8	25	0.67
<80	10 (26)	10.0	11		10 (26)	29.2	27	
Gross total resection								
Yes	18 (46)	23.8	11	0.32	18 (46)	43.2	26	0.29
No	21 (54)	0	13		21 (54)	9.7	27	
Ki-67 labeling index								
<15%	12 (44)	16.7	21.5	**0.049**	12 (44)	33.3	30.5	0.16
≥15%	15 (56)	0	10		15 (56)	25.6	17	
TP53								
Wild-type	24 (62)	9.9	11	0.98	24 (62)	33.8	34	0.16
Mutated	15 (38)	10.0	17		15 (38)	12.5	25	
1p/19q codeletion								
Yes	4 (10)	33.3	47	0.095	4 (10)	66.7	NR	0.099
No	35 (90)	7.8	11		35 (90)	21.7	22	
Gain of 7p								
No	26 (67)	12.0	11	0.80	26 (67)	38.4	34	0.28
Yes	13 (33)	7.7	13		13 (33)	9.9	22	
Homozygous deletion of 9p								
No	33 (85)	8.5	11	0.93	33 (85)	24.6	26	0.67
Yes	6 (15)	16.7	13		6 (15)	33.3	16	
Loss of 10q								
No	35 (90)	11.5	13	0.086	35 (90)	28.7	26	0.22
Yes	4 (10)	0	8.5		4 (10)	0	20.5	
MGMT								
Methylated	18 (44)	11.8	17	0.48	18 (44)	26.6	25	0.61
Unmethylated	21 (56)	8.4	11		21 (56)	24.0	26	

AA anaplastic astrocytoma, *AO* anaplastic oligodendroglioma, *AOA* anaplastic oligoastrocytoma, *OS* overall survival, *PFS* progression-free survival

Bold indicates statistical significance at $P < 0.050$

deletion of 9p, and 33% of *EGFR* amplification (only one case of truncated variant of *EGFR*) (Tables 2, 6), which were less frequent compared to the majority of glioblastoma carrying 69% of 10q loss [30], 31–57% of homozygous deletion of 9p [30, 31], and 34–39% of *EGFR* amplification (20–50% were truncated variants) [24, 30, 32, 33]. These observations indicate that grade III glioma with wild-type *IDH1/2* is distinct from both grade III

glioma with mutated *IDH1/2* and glioblastoma, and thus cannot be categorized into the current WHO classification. This fact was supported by the evidence that the frequency of *IDH1/2* gene mutation in grade III gliomas (62–69.1%) is lower than that in grade II gliomas (71–82%) [1, 3, 4, 28], indicating that some grade III gliomas may develop through a bypass pathway without *IDH1/2* gene mutation.

In conclusion, subgroup analysis of the clinical and genetic profiles of grade III gliomas by *IDH1/2* gene status helped to understand their concealed background. Grade III glioma patients with *IDH1/2* mutation present favorable prognosis; however, careful follow-up is needed in patients with incomplete resection, 7p gain, and *TP53* gene mutation. Grade III glioma patients with wild-type *IDH1/2* present poor prognosis; however, oligodendroglial component and 1p19q codeletion tend to show better prognosis even in this unfortunate group. These facts may help predict the prognosis of patients with grade III glioma precisely, and be a supportive factor in histological diagnosis.

Acknowledgments This work was supported in part by Grants-in-Aid for Cancer Research from the Ministry of Health and Welfare in Japan to T. T. We thank T. Matsuki and M. Fue for assistance in extracting genomic DNA and PCR analysis.

Conflict of interest There is no conflict of interest to declare.

References

1. Balss J, Meyer J, Mueller W et al (2008) Analysis of the IDH1 codon 132 mutation in brain tumors. Acta Neuropathol 116(6): 597–602
2. Parsons DW, Jones S, Zhang X et al (2008) An integrated genomic analysis of human glioblastoma multiforme. Science 321(5897):1807–1812
3. Yan H, Parsons DW, Jin G et al (2009) IDH1 and IDH2 mutations in gliomas. N Engl J Med 360(8):765–773
4. Watanabe T, Nobusawa S, Kleihues P et al (2009) IDH1 mutations are early events in the development of astrocytomas and oligodendrogliomas. Am J Pathol 174(4):1149–1153
5. Ohgaki H, Kleihues P (2009) Genetic alterations and signaling pathways in the evolution of gliomas. Cancer Sci 100(12):2235–2241
6. Yan H, Bigner DD, Velculescu V et al (2009) Mutant metabolic enzymes are at the origin of gliomas. Cancer Res 69(24):9157–9159
7. van den Bent MJ, Dubbink HJ, Marie Y et al (2010) IDH1 and IDH2 mutations are prognostic but not predictive for outcome in anaplastic oligodendroglial tumors: a report of the European Organization for Research and Treatment of Cancer Brain Tumor Group. Clin Cancer Res 16(5):1597–1604
8. Ichimura K, Pearson DM, Kocialkowski S et al (2009) IDH1 mutations are present in the majority of common adult gliomas but rare in primary glioblastomas. Neuro Oncol 11(4): 341–347
9. Levin VA, Hess KR, Choucair A et al (2003) Phase III randomized study of postradiotherapy chemotherapy with combination alpha-difluoromethylornithine-PCV versus PCV for anaplastic gliomas. Clin Cancer Res 9(3):981–990
10. van den Bent MJ, Carpentier AF, Brandes AA et al (2006) Adjuvant procarbazine, lomustine, and vincristine improves progression-free survival but not overall survival in newly diagnosed anaplastic oligodendrogliomas and oligoastrocytomas: a randomized European Organisation for Research and Treatment of Cancer phase III trial. J Clin Oncol 24(18):2715–2722
11. Sanson M, Marie Y, Paris S et al (2009) Isocitrate dehydrogenase 1 codon 132 mutation is an important prognostic biomarker in gliomas. J Clin Oncol 27(25):4150–4154
12. Houillier C, Mokhtari K, Carpentier C et al (2010) Chromosome 9p and 10q losses predict unfavorable outcome in low-grade gliomas. Neuro Oncol 12(1):2–6
13. Sonoda Y, Kumabe T, Nakamura T et al (2009) Analysis of IDH1 and IDH2 mutations in Japanese glioma patients. Cancer Sci 100(10):1996–1998
14. Mashiyama S, Murakami Y, Yoshimoto T et al (1991) Detection of p53 gene mutations in human brain tumors by single-strand conformation polymorphism analysis of polymerase chain reaction products. Oncogene 6(8):1313–1318
15. Sonoda Y, Kumabe T, Watanabe M et al (2009) Long-term survivors of glioblastoma: clinical features and molecular analysis. Acta Neurochir (Wien) 151(11):1349–1358
16. Sonoda Y, Yokosawa M, Saito R, et al (2010) O(6)-Methylguanine DNA methyltransferase determined by promoter hypermethylation and immunohistochemical expression is correlated with progression-free survival in patients with glioblastoma. Int J Clin Oncol 15:352–358
17. Wick W, Hartmann C, Engel C et al (2009) NOA-04 randomized phase III trial of sequential radiochemotherapy of anaplastic glioma with procarbazine, lomustine, and vincristine or temozolomide. J Clin Oncol 27(35):5874–5880
18. Jeuken J, Sijben A, Alenda C et al (2009) Robust detection of EGFR copy number changes and EGFR variant III: technical aspects and relevance for glioma diagnostics. Brain Pathol 19(4):661–671
19. Jeuken J, Cornelissen S, Boots-Sprenger S et al (2006) Multiplex ligation-dependent probe amplification: a diagnostic tool for simultaneous identification of different genetic markers in glial tumors. J Mol Diagn 8(4):433–443
20. Jeuken JW, Cornelissen SJ, Vriezen M et al (2007) MS-MLPA: an attractive alternative laboratory assay for robust, reliable, and semiquantitative detection of MGMT promoter hypermethylation in gliomas. Lab Invest 87(10):1055–1065
21. Kato H, Kato S, Kumabe T et al (2000) Functional evaluation of p53 and PTEN gene mutations in gliomas. Clin Cancer Res 6(10):3937–3943
22. Kanamori M, Kumabe T, Sonoda Y et al (2009) Predictive factors for overall and progression-free survival, and dissemination in oligodendroglial tumors. J Neurooncol 93(2):219–228
23. Ohgaki H, Kleihues P (2005) Population-based studies on incidence, survival rates, and genetic alterations in astrocytic and oligodendroglial gliomas. J Neuropathol Exp Neurol 64(6): 479–489
24. Smith JS, Tachibana I, Passe SM et al (2001) PTEN mutation, EGFR amplification, and outcome in patients with anaplastic astrocytoma and glioblastoma multiforme. J Natl Cancer Inst 93(16):1246–1256
25. Dehais C, Laigle-Donadey F, Marie Y et al (2006) Prognostic stratification of patients with anaplastic gliomas according to genetic profile. Cancer 107(8):1891–1897
26. Etienne MC, Formento JL, Lebrun-Frenay C et al (1998) Epidermal growth factor receptor and labeling index are independent prognostic factors in glial tumor outcome. Clin Cancer Res 4(10):2383–2390

27. Zhou YH, Tan F, Hess KR et al (2003) The expression of PAX6, PTEN, vascular endothelial growth factor, and epidermal growth factor receptor in gliomas: relationship to tumor grade and survival. Clin Cancer Res 9(9):3369–3375
28. Hartmann C, Meyer J, Balss J et al (2009) Type and frequency of IDH1 and IDH2 mutations are related to astrocytic and oligodendroglial differentiation and age: a study of 1,010 diffuse gliomas. Acta Neuropathol 118(4):469–474
29. Weller M, Felsberg J, Hartmann C et al (2009) Molecular predictors of progression-free and overall survival in patients with newly diagnosed glioblastoma: a prospective translational study of the German Glioma Network. J Clin Oncol 27(34):5743–5750
30. Ohgaki H, Dessen P, Jourde B et al (2004) Genetic pathways to glioblastoma: a population-based study. Cancer Res 64(19): 6892–6899
31. Ueki K, Ono Y, Henson JW et al (1996) CDKN2/p16 or RB alterations occur in the majority of glioblastomas and are inversely correlated. Cancer Res 56(1):150–153
32. Gan HK, Kaye AH, Luwor RB (2009) The EGFRvIII variant in glioblastoma multiforme. J Clin Neurosci 16(6):748–754
33. Aldape KD, Ballman K, Furth A et al (2004) Immunohistochemical detection of EGFRvIII in high malignancy grade astrocytomas and evaluation of prognostic significance. J Neuropathol Exp Neurol 63(7):700–707

Cancer Letters 310 (2011) 77–83

Contents lists available at ScienceDirect

Cancer Letters

journal homepage: www.elsevier.com/locate/canlet

Local convection-enhanced delivery of chemotherapeutic agent transiently opens blood–brain barrier and improves efficacy of systemic chemotherapy in intracranial xenograft tumor model

Taigen Nakamura, Ryuta Saito *, Shin-ichiro Sugiyama, Yukihiko Sonoda, Toshihiro Kumabe, Teiji Tominaga

Department of Neurosurgery, Tohoku University Graduate School of Medicine, Sendai, Miyagi, Japan

ARTICLE INFO

Article history:
Received 15 February 2011
Received in revised form 2 June 2011
Accepted 12 June 2011

Keywords:
Convection-enhanced delivery
Local chemotherapy
Blood–brain barrier
Brain tumor
ACNU

ABSTRACT

Recently, local chemotherapy proved its efficacy against malignant gliomas. Under the hypothesis that local delivery of chemotherapeutic agents into the brain parenchyma induce opening of the blood–brain barrier (BBB), we evaluated the opening of BBB after convection-enhanced delivery of nimustine hydrochloride into the brain parenchyma. Local convection-enhanced delivery of nimustine hydrochloride transiently opened the BBB from about 7–12 days after delivery in normal rodent brain. Systemic chemotherapy during this period of BBB disruption had synergistic effects resulting in prolonged survival of tumor-bearing rats. The present strategy may provide a new approach for glioma chemotherapy.

1. Introduction

Glioblastoma is the most common and most aggressive type of primary brain tumor. Approximately 3 in 100,000 people in the US and European countries are diagnosed with glioblastoma every year, and the median survival of a patient with glioblastoma is 15 months [1]. Only a minority of patients live longer than 3 years because therapies for the treatment of glioblastoma have only limited effectiveness despite the best efforts of researchers [2]. Post-surgical placement of small biodegradable polymer wafers designed to deliver carmustine (BCNU) directly into the resection cavity provides a survival benefit in patients with newly diagnosed and recurrent glioblastoma [3,4]. This procedure illustrates the therapeutic potential of extensive local chemotherapy against this devastating disease.

The emergence of effective cancer chemotherapy is one of the major medical advances of the second half of the 20th century [5]. New lineups of chemotherapeutic agents and molecular targeted agents have been introduced to treat neoplasms. However, patients with gliomas fail to receive the benefits provided by most of these agents. Temozolomide is the only agent that has demonstrated therapeutic efficacy [6]. The properties of the blood–brain barrier (BBB), although compromised to some extent in glioblastomas, may be the reason for this failure [7]. Poor penetration of most anticancer drugs across the BBB and into the central nervous system is well documented. Even drugs that penetrate the BBB cannot reach adequate drug concentrations in brain-tumor tissue without causing systemic side effects [7]. Therefore, methods to transiently open this barrier have been extensively studied, including osmotic disruption using hyperosmotic shock [8], and biochemical disruption by administration of vasoactive substances [9].

Local drug delivery to the affected brain location should theoretically bypass the BBB, reduce systemic drug levels to minimize the side effects of chemotherapy, and provide

* Corresponding author. Address: Department of Neurosurgery, Tohoku University Graduate School of Medicine, 1-1 Seiryo-machi, Aoba-ku, Sendai, Miyagi 980-8574, Japan. Tel.: +81 22 717 7230; fax: +81 22 717 7233.

E-mail address: ryuta@nsg.med.tohoku.ac.jp (R. Saito).

0304-3835/$ - see front matter © 2011 Elsevier Ireland Ltd. All rights reserved.
doi:10.1016/j.canlet.2011.06.018

prolonged higher levels of intracerebral chemotherapeutic agents relative to those obtainable by systemic administration [7,10]. However, for many local drug-delivery technologies including simple intratumoral injection or polymer implantation, the ultimate efficacy depends on the diffusion of the drugs into the brain parenchyma. An important advance in local drug delivery is the development of convection-enhanced delivery (CED) [11]. This technique uses bulk flow to directly deliver small or large molecules to targeted sites in clinically significant volumes of tissue, resulting in improved volumes of distribution compared with simple diffusion techniques [10]. This technique is now being applied to deliver BCNU [12], topotecan [13], carboplatin, gemcitabine [14], and paclitaxel [15] to brain tumors, all with promising outcomes.

Recently, we have been investigating the CED of nimustine hydrochloride (ACNU) as a new strategy to effectively treat glioblastoma [16–18]. During our study, we observed a period when the brain treated with ACNU becomes enhanced on magnetic resonance imaging after intravenous administration of contrast agents, suggesting that the BBB becomes leaky after local administration of chemotherapeutic agent. In the present study, we tried to identify this leaky period, and investigated whether the efficacy of combination systemic chemotherapy was enhanced during this period.

2. Materials and methods

2.1. Pegylated (polyethylene glycol-coated) liposomal doxorubicin (PLD) and ACNU

PLD (Doxil; Alza Pharmaceuticals, Mountain View, CA) was obtained commercially. The commercial PLD solution contained 2 mg/mL of doxorubicin. ACNU was provided by Daiichi-Sankyo Co. Ltd. (Tokyo, Japan). Infusion solutions of ACNU were prepared by diluting ACNU in 0.9% NaCl solution to a concentration of 1 mg/mL.

2.2. Tumor cell line, animals, and intracranial xenograft technique

The 9 L rat gliosarcoma cells (American Type Culture Collection, Rockville, MD) were maintained as monolayers in a complete medium consisting of Eagle's minimal essential medium supplemented with 10% fetal bovine serum, non-essential amino acids, and 100 U/mL penicillin G. Cells were cultured at 37 °C in a humidified atmosphere consisting of 95% air and 5% CO_2. Male Sprague–Dawley rats weighting approximately 200 g were purchased from Charles-River Japan Laboratories (Tsukuba, Ibaraki, Japan). Male Fisher 344 rats weighting approximately 200 g were purchased from Kumagai-Shigeyasu Co., Ltd. (Sendai, Miyagi, Japan). All protocols used for the animal studies were approved by the Institute for Animal Experimentation of Tohoku University Graduate School of Medicine. To establish the intracranial xenograft tumor model, cells were harvested by trypsinization, washed once with Hanks' balanced salt solution without Ca^{2+} and Mg^{2+} (HBSS), and resuspended in HBSS for implantation. A cell suspension containing 5×10^5 cells/10 μL HBSS was used for implantation into the striatal region of the Fisher 344 rat brains. Under deep halothane anesthesia, rats were placed in a small-animal stereotactic frame (David Kopf Instrument, Tujunga, CA). A sagittal incision was made to expose the cranium followed by a burr hole in the skull located at 0.5 mm anterior and 3 mm lateral from the bregma using a small dental drill. Cell suspension (5 μL) was injected over 2 min at a depth of 4.5 mm from the brain surface; after a 2-min wait, another 5 μL was injected over 2 min at a depth of 4.0 mm; and after a final 2-min wait, the needle was removed and the wound was sutured.

2.3. Convection-enhanced delivery

CED with a volume of 20 μL of ACNU or PBS was performed as described previously [19,20]. Briefly, the infusion system consisted of a reflux-free, step-design infusion cannula connected to a loading line (containing ACNU or PBS (GIBCO™ PBS; Life technologies Japan Ltd., Tokyo, Japan)) and an olive oil infusion line. A 1-mL syringe (filled with oil) mounted onto a micro-infusion pump (BeeHive; Bioanalytical Systems, West Lafayette, IN) regulated the flow of fluid through the system. Based on chosen coordinates, the infusion cannula was mounted onto stereotactic holders and guided to the target region of the brain through burr holes made in the skull. The following ascending infusion rates were applied to achieve 20 μL infusion: 0.2 μL/min (15 min) + 0.5 μL/min (10 min) + 0.8 μL/min (15 min).

2.4. Evaluation of toxicity

Three healthy male Sprague–Dawley rats weighing approximately 200 g received a single 20 μL CED infusion of 1 mg/mL ACNU. Rats were monitored daily for survival, weekly weights, and general health. Rats were euthanized on the 60th day after the CED, and their brains were removed, fixed, subjected to paraffin sectioning (5 μm), and stained with hematoxylin and eosin.

2.5. Volumetric evaluation of BBB disruption

Twenty normal male Fisher 344 rats weighting approximately 200 g received a single 20 μL CED infusion of 1 mg/mL ACNU and were randomly assigned to five groups. In each group of four rats, 1 mL of 2% Evans blue solution (Sigma–Aldrich, Tokyo, Japan) in saline was administered through the tail veins at 3, 7, 12, 20, and 30 days after CED. Rats were euthanized 30 min after administration. After transcardial perfusion with NaCl solution, their brains were harvested, frozen with ice-cold isopentane, and cut into serial coronal sections (25 μm) with a cryostat. Evans blue generates fluorescence under UV illumination, so the areas of brain section containing extravasated Evans blue were visualized using a fluorescence microscope, and a charged-coupled device camera with a fixed aperture was used to capture the image. The volumes of brain that contained extravasated Evans blue were calculated from these images.

2.6. Quantitative evaluation of BBB disruption

Twenty-four normal male Fisher 344 rats weighing approximately 200 g received a single 20 μL CED infusion of 1 mg/mL ACNU. As for volumetric analysis, 1 mL of 4% Evans blue solution was administered to Fisher 344 rats 3 (n = 9), 7 (n = 9), and 30 (n = 6) days after CED. Rats were euthanized 30 min after Evans blue administration. After transcardial perfusion with NaCl solution, their brains were harvested. Extravasation of Evans blue in the hemispheres (3 mm anterior and 3 mm posterior from the CED point) was measured according to the method of Chan et al. [21,22]. After homogenization with 1 mL PBS, samples were centrifuged at 1000g for 30 min. Supernatants (0.7 mL) were taken, and an equal volume of 100% trichloroacetic acid was added to precipitate protein. The samples were allowed to stand overnight at 4 °C, and were then centrifuged at 1000g for 30 min. The absorbance of Evans blue at 610 nm was measured in the supernatants using a spectrophotometer. Evans blue content was expressed as μg per hemisphere calculated against a standard.

2.7. Extravasation of PLD after CED in intracranial xenograft tumor model

Six male Fisher 344 rats with intracranial xenograft tumors were used for this study. Five days after tumor implantation, three rats received CED of ACNU (0.1 mg/mL, 20 μL), and three rats received CED of 20 μL PBS. Seven days after CED, all rats received bolus intravenous injections of 1 mL PLD solution (2.0 mg/mL) via the tail veins. Thirty minutes after PLD administration, rats were perfused transcardially with NaCl solution. Brains were harvested and frozen with ice-cold isopentane, and cut into serial coronal sections (25 μm) with a cryostat. PLD generates fluorescence under UV illumination, so the areas of brain section containing extravasated PLD were visualized using a fluorescence microscope, and a charged-coupled device camera with a fixed aperture was used to capture the image. The same sections were then stained with hematoxylin and eosin.

2.8. Survival study using the intracranial xenograft model

Forty-two male Fisher 344 rats with intracranial xenograft tumors were randomly assigned to five groups as summarized in Table 1: (a) control group received CED of PBS (n = 9), (b) group received intravenous PLD administration after CED of PBS (n = 9), (c) group received CED of ACNU (n = 8), (d) group received intravenous PLD administration after CED of ACNU (n = 9); and (e) group received CED of ACNU after intravenous PLD administration (n = 7). Five days after tumor cell implantation (Day 5), single CED infusions (20 μL infusion of 1 mg/mL ACNU or PBS) were performed for groups (a, b, c, and d), and bolus intravenous injections of 400 μL PLD (2.0 mg/mL) via the tail veins were performed for group (e). Seven days later (Day 12), bolus intravenous injections of 400 μL PLD (2.0 mg/mL) via the tail veins were performed for groups (b, d, and e). Six days later (Day 18), bolus intravenous injections of 400 μL PLD (2.0 mg/mL) via the tail veins were performed for groups (b and d), and CED infusions (20 μL of 1 mg/mL ACNU) were performed for group (e). The dose of PLD used in this study was selected based on previous studies [23,24]. Survival was expressed as a Kaplan–Meier curve. Survival was compared between the treatment groups with a log-rank test.

3. Results

3.1. Negligible local toxicity of 1 mg/mL ACNU delivered via CED

CED infusion of 20 μL ACNU at concentration of 1 mg/mL caused little local tissue damage when infused into normal rat hemisphere (Fig. 1), as previously reported [16,17]. Slight tissue damage was noted only at the needle tract without obvious tissue damage in the surrounding brain that received ACNU. Even at higher magnification, no strong inflammatory response or tissue necrosis was detected. No rat developed neurological deficit or lost their weight. This dose of ACNU (20 μL of 1 mg/mL ACNU) was used throughout this study.

3.2. Extravasation of intravenous Evans blue 7 days after CED of ACNU

Although CED of ACNU caused little local tissue change as described above, leakage of intravenously infused 2% Evans blue solution was observed 7 days after CED of ACNU into the hemispheres of normal Fisher 344 rats. Representative brain sections are shown in Fig. 2A. Fluorescent microscopy detected Evans blue in the brain parenchyma indicating leakage from the BBB. In contrast, leakage of Evans blue was hardly observed 7 days after CED of PBS (Fig. 2B). Results were similar for all four rats tested.

3.3. Transient disruption of BBB after CED of ACNU

To test the time course of BBB disruption, leakage of intravenously infused Evans blue solution was evaluated 3, 7, 12, 20, and 30 days after CED of ACNU using fluorescent images. The leakage of Evans blue was small 3 days after CED, but became prominent from 7 to 12 days after CED, and then diminished (Fig. 3). Volumetric analysis of the fluorescent area confirmed the findings.

3.4. Quantitative analysis of transient disruption of BBB after CED of ACNU

Quantitative spectrophotometric analysis of Evans blue leakage through the disrupted BBB compared the amount of Evans blue in the brains of rats 3, 7, and 30 days after CED of ACNU. Brains of rats contained

Table 1
Five groups for survival study using the intracranial xenograft model.

Group	n	Day 0	Day 5	Day 12	Day 18
(a) Control	9	Implantation	PBS CED	PBS iv	PBS iv
(b) PLD iv	9	Implantation	PBS CED	PLD iv	PLD iv
(c) ACNU CED	8	Implantation	ACNU CED	PBS iv	PBS iv
(d) ACNU CED + PLD iv	9	Implantation	ACNU CED	PLD iv	PLD iv
(e) PLD iv + ACNU CED	7	Implantation	PLD iv	PLD iv	ACNU CED

Abbreviations: iv = intravenous, CED = convection-enhanced delivery, PLD = pegylated liposomal doxorubicin, PBS = phosphate buffered saline.

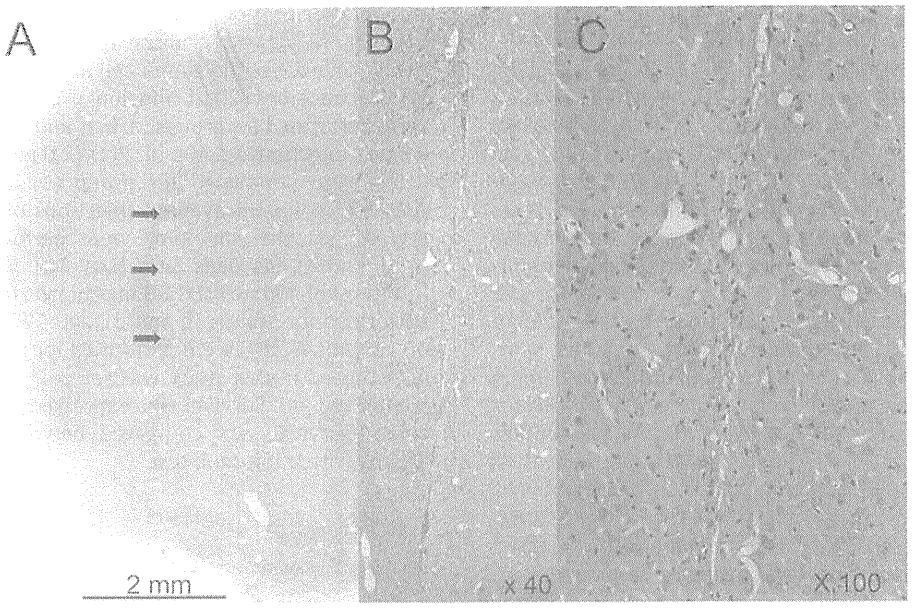

Fig. 1. Local tissue toxicity of ACNU administered via CED in the normal adult rat brain. Rat brains were treated with a single CED infusion of 20 μL of 1.0 mg/mL ACNU. Representative hematoxylin and eosin sections from rats euthanized 30 days after CED. Rats showed no drug-induced damage (A). Arrows indicate the needle tract. Higher magnification of tissue around needle tract (B: ×40, C: ×100).

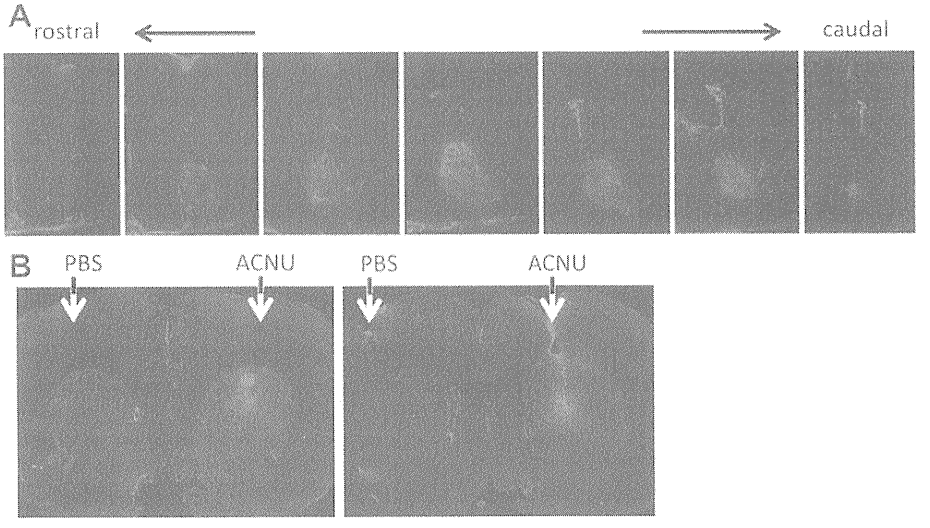

Fig. 2. Seven days after CED of ACNU into the hemisphere of normal Fisher 344 rats, 2% Evans blue solution was injected via the tail vein. Rats were euthanized 30 min after Evans blue administration. After transcardial perfusion with NaCl solution, their brains were harvested, frozen, and cut into serial coronal sections (25 μm) with a cryostat. Brain sections were observed with a fluorescence microscope to detect the extravasation of Evans blue. Sequential brain sections at 500-μm intervals from a representative rat are shown (A). Sequential brain sections at 500-μm intervals of another rat that received tail vein injection of 2% Evans blue 7 days after CED of ACNU into one hemisphere and CED of PBS into the other hemisphere (B).

significantly higher amount of Evans blue 7 days after CED than on other days (Fig. 4), which confirmed the findings of the volumetric analysis.

3.5. Disruption of BBB after CED of ACNU in xenograft tumor model

Tumor vessels are usually more leaky than normal vessels. BBB disruption was evaluated in the intracranial xenograft tumor model. Seven days after CED of ACNU ($n = 3$) or PBS ($n = 3$), PLD was injected from the tail vein. Although mild leakage was observed in rats that received CED of PBS, leakage was more extensive in rats that received CED of ACNU (Fig. 5). One of three rats that received CED of ACNU harbored two separate tumors located just at the needle tract of ACNU infusion and at a deeper location probably not reached by infused ACNU. This enabled us to evaluate the efficacy of infused ACNU. Leakage of PLD was more prominent in the tumor located at the needle tract compared to the deeply located tumor. With the hypothesis that this leakage of PLD after CED of ACNU may benefit the survival of brain tumor xenografts, we conducted the following survival study.

3.6. Survival study

Survival study is summarized as a Kaplan–Meier curve (Fig. 6). CED of ACNU ($P = 0.017$; log-rank test) but not PLD ($P = 0.26$) prolonged the survival of tumor-bearing rats. Survival was improved when CED of ACNU

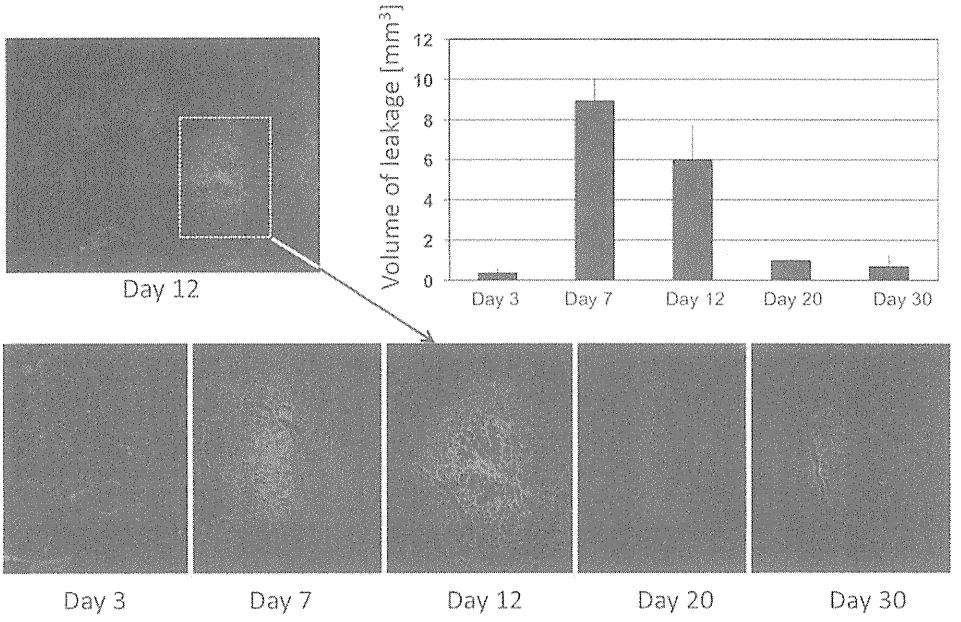

Fig. 3. Leakage of intravenously infused Evans blue solution 3, 7, 12, 20, and 30 days after CED of ACNU. Brains were processed as in Fig. 2 and observed under a fluorescence microscope. Representative image from rat brain that received Evans blue 12 days after CED (upper left). Lower images depict the magnified images of the boxed area from each day period. The fluorescence images were acquired under the same conditions. Volumetric analysis of the area that contained fluorescence from Evans blue (upper right). Bars at top of each column indicate the standard deviation.

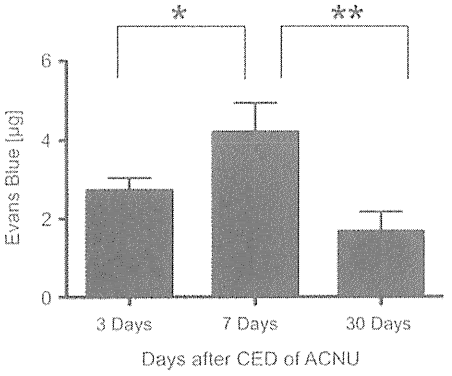

Fig. 4. Evans blue content in the brains of rats that received intravenous injection of 4% Evans blue solution 3, 7, and 30 days after CED of ACNU was measured using a spectrophotometer. Evans blue content was expressed as μg per hemisphere calculated against a standard. Bars at top of each column indicate the standard deviation. $^{*}P = 0.042$, $^{**}P = 0.013$, Student *t*-test.

was given prior to PLD ($P = 0.0001$; compared with control, $P = 0.003$; compared with CED of ACNU alone), but not when PLD was given prior to CED of ACNU ($P = 0.27$; compared with control). BBB disruption caused by CED of ACNU may be one reason for this improved survival.

4. Discussion

Our previous studies reported the safety and efficacy of CED of ACNU in the intracranial xenograft tumor model [16,17]. The present study confirmed that CED of 1 mg/mL ACNU produced no severe toxicity (Fig. 1). However, disruption of the BBB was observed. Qualitative evaluation revealed robust distribution of Evans blue in the normal rat hemisphere after intravenous administration, which was confirmed by quantitative evaluation.

Local chemotherapy can be effective against malignant gliomas, and CED can deliver drugs much more extensively into the target region, but may have some limitations. The vast majority of neoplastic cells in malignant gliomas are found within the tumor bed and within 2 cm of the enhanced borders, but migrating cells can be found several centimeters away from the tumor and even in the contralateral hemisphere [25]. Moreover, dissemination limits the survival of patients with locally well controlled malignant gliomas [26]. Therefore, effective local therapy should be administered together with effective systemic therapy. However, systemic chemotherapy is limited because 98% of small molecules and 100% of large molecules cannot cross the BBB [27]. Many promising agents including molecular targeted agents have not been as effective as expected.

In this context, our findings provide the rationale for combining local and systemic chemotherapy. The observed BBB disruption after local chemotherapy was reversible. Leakage was observed only between 1 and 2 weeks after delivery of ACNU. The exact mechanism for this transient disruption of the BBB is not clear, but slight disturbance of the BBB caused by chemotherapeutic agents is likely to recover fairly rapidly. In this study, delivery of intravenous Evans blue or PLD was augmented during this time window, but not later. Therefore, this transient dysfunction of the BBB gives a time window for effective delivery of systemic chemotherapeutic agents.

Drug delivery to brain tumors has been a controversial subject. Some researchers believe that the BBB is not

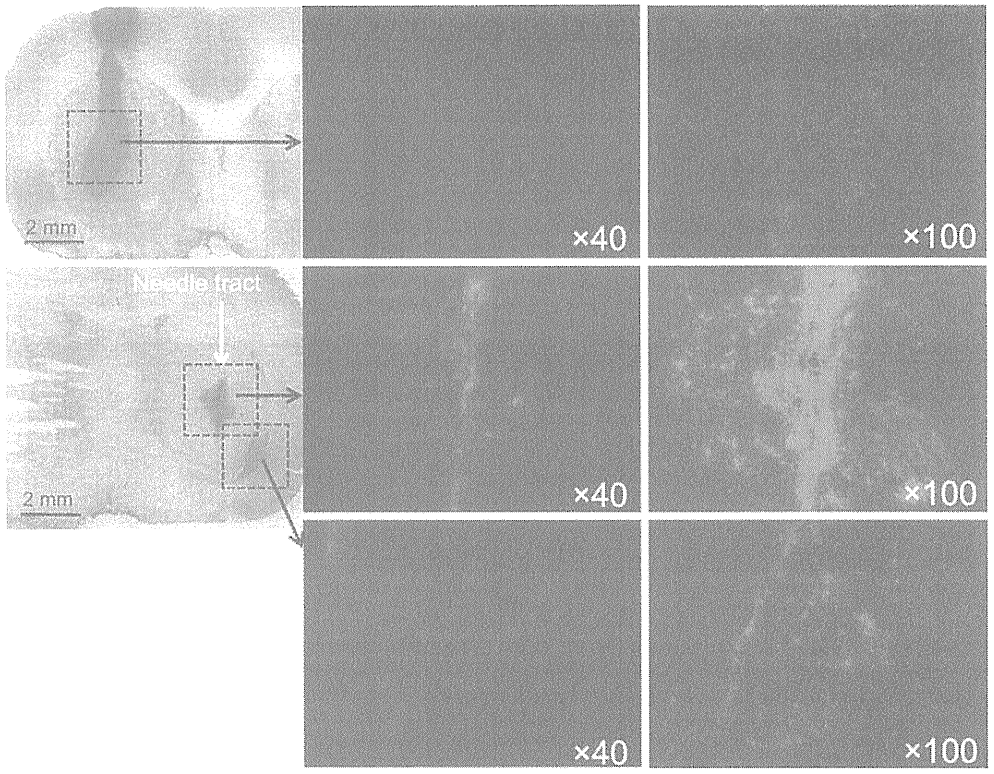

Fig. 5. Seven days after CED of ACNU ($n = 3$) or PBS ($n = 3$), PLD was injected via the tail vein. Although mild leakage was observed in rats that received CED of PBS (upper row), leakage was more extensive in rats that received CED of ACNU (middle and lower row). One of three rats that received CED of ACNU had two separate tumors, located just at the needle tract of ACNU infusion and at a deeper location probably not reached by infused ACNU. Leakage of PLD was more prominent in the tumor located at the needle tract (middle row) compared to the deeply located tumor (lower row).

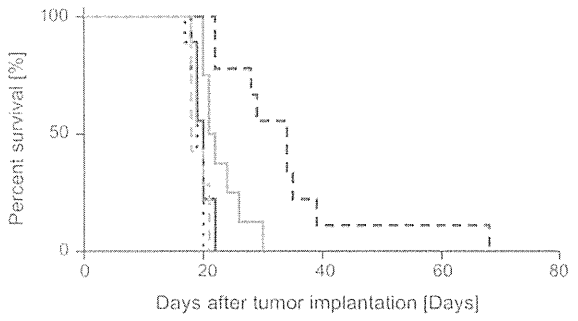

Fig. 6. Survival of the five groups expressed as a Kaplan–Meier curve. Black solid line, (a) control; black dotted line, (b) intravenous PLD; gray solid line, (c) CED of ACNU; black dashed line, (d) CED of ACNU plus intravenous PLD; and gray dashed line, (e) intravenous PLD plus CED of ACNU.

important, while others believe it is the major obstacle in treatment [28]. However, on the whole, the understanding is that the BBB and the blood–tumor barrier prevent drugs from reaching brain tumors in sufficient concentrations to kill the tumor cells [7]. In this study, we evaluated the leakage of PLD into the xenograft brain tumor model. Permeability of experimental gliomas is reported to be 10^4–10^5 higher than the normal brain if the molecular size of the agent is small enough [29]. Fluorescence from PLD was observed in the tumors, but the fluorescence was obviously more intense after infusion of ACNU. The survival study also demonstrated the efficacy of the combination of ACNU CED and intravenous PLD, but only if intravenous PLD was given during the period of BBB disruption. This combination significantly prolonged survival of the tumor model rats if intravenous PLD was given 5 and 12 days after CED of ACNU. This efficacy was not observed if the agents were used in the opposite order. Moreover, the group treated by CED of ACNU following intravenous administration of PLD did not survive longer than the control group while the group treated by CED of ACNU had significantly longer survival than the control group. This may be because that xenografted tumors 18 days after implantation become too large to be treated by CED of 20 μL ACNU although intravenous PLD was given 5 and 12 days after implantation.

Many methods have been assessed to transiently disrupt the BBB for effective drug delivery to the central nervous system. Osmotic disruption such as hyperosmotic shock, and biochemical disruption induced by administration of vasoactive substances have been tested [8,9,27]. Tumor chemotherapy combined with these BBB opening agents seemed promising at first, but were abandoned because of the potential for structural brain damage in areas of BBB disruption. Compared with these strategies, the present method disrupts the BBB only at the site of drug

distribution achieved by CED. As the CED of chemotherapeutic agents targets the site of tumor invasion, this method may be effective without severe toxicity to other parts of the brain.

The present study showed that local application of chemotherapeutic agents into the brain parenchyma induced transient opening of the BBB. Systemic chemotherapy during this period of BBB disruption had synergistic effects resulting in prolonged survival of tumor-bearing rats. The present strategy may provide a new approach for glioma chemotherapy.

Conflict of interest

None declared.

Acknowledgements

This work was supported in part by Grants-in-Aid for Scientific Research from the Ministry of Health, Labour and Welfare in Japan to R.S. (Grant No. 21791341, 2009).

References

[1] A. Jemal, T. Murray, A. Samuels, A. Ghafoor, E. Ward, M.J. Thun, Cancer statistics 2003, CA Cancer J. Clin. 53 (2003) 5–26.
[2] A.A. Brandes, State-of-the-art treatment of high-grade brain tumors, Semin. Oncol. 30 (6 Suppl. 19) (2003) 4–9.
[3] S. Gururangan, L. Cokgor, J.N. Rich, S. Edwards, M.L. Affronti, J.A. Quinn, J.E. Herndon 2nd, J.M. Provenzale, R.E. McLendon, S. Tourt-Uhlig, J.H. Sampson, V. Stafford-Fox, S. Zaknoen, M. Early, A.H. Friedman, H.S. Friedman, Phase I study of Gliadel wafers plus temozolomide in adults with recurrent supratentorial high-grade gliomas, Neurol. Oncol. 3 (2001) 246–250.
[4] M. Westphal, D.C. Hilt, E. Bortey, P. Delavault, R. Olivares, P.C. Warnke, I.R. Whittle, J. Jääskeläinen, Z. Ram, A phase 3 trial of local chemotherapy with biodegradable carmustine (BCNU) wafers (Gliadel wafers) in patients with primary malignant glioma, Neurol. Oncol. 5 (2003) 79–88.
[5] M.R. Green, Targeting targeted therapy, New Engl. J. Med. 350 (2004) 2191–2193.
[6] R. Stupp, W.P. Mason, M.J. van den Bent, M. Weller, B. Fisher, M.J. Taphoorn, K. Belanger, A.A. Brandes, C. Marosi, U. Bogdahn, J. Curschmann, R.C. Janzer, S.K. Ludwin, T. Gorlia, A. Allgeier, D. Lacombe, J.G. Cairncross, E. Eisenhauer, R.O. Mirimanoff, European Organisation for Research and Treatment of Cancer Brain Tumor and Radiotherapy Groups, National Cancer Institute of Canada Clinical Trials Group, Radiotherapy plus concomitant and adjuvant temozolomide for glioblastoma, New Engl. J. Med. 352 (2005) 987–996.
[7] D.R. Groothuis, The blood–brain and blood–tumor barriers: a review of strategies for increasing drug delivery, Neurol. Oncol. 2 (2000) 45–59.
[8] R.A. Kroll, E.A. Neuwelt, Outwitting the blood–brain barrier for therapeutic purposes: osmotic opening and other means, Neurosurgery 42 (1998) 1083–1099.
[9] K. Matsukado, T. Inamura, S. Nakano, M. Fukui, R.T. Bartus, K.L. Black, Enhanced tumor uptake of carboplatin and survival in glioma-bearing rats by intracarotid infusion of bradykinin analog, RMP-7, Neurosurgery 39 (1996) 125–133.
[10] K.A. Walter, R.J. Tamargo, A. Olivi, P.C. Burger, H. Brem, Intratumoral chemotherapy, Neurosurgery 37 (1995) 1128–1145.
[11] R.H. Bobo, D.W. Laske, A. Akbasak, P.F. Morrison, R.L. Dedrick, E.H. Oldfield, Convection-enhanced delivery of macromolecules in the brain, Proc. Natl. Acad. Sci. USA 91 (1994) 2076–2080.
[12] J.N. Bruce, A. Falavigna, J.P. Johnson, J.S. Hall, B.D. Birch, J.T. Yoon, E.X. Wu, R.L. Fine, A.T. Parsa, Intracerebral clysis in a rat glioma model, Neurosurgery 46 (2000) 683–691.
[13] M.G. Kaiser, A.T. Parsa, R.L. Fine, J.S. Hall, I. Chakrabarti, J.N. Bruce, Tissue distribution and antitumor activity of topotecan delivered by intracerebral clysis in a rat glioma model, Neurosurgery 47 (2000) 1391–1399.
[14] J.W. Degen, S. Walbridge, A.O. Vortmeyer, E.H. Oldfield, R.R. Lonser, Safety and efficacy of convection-enhanced delivery of gemcitabine or carboplatin in a malignant glioma model in rats, J. Neurosurg. 99 (2003) 893–898.
[15] Z. Lidar, Y. Mardor, T. Jonas, R. Pfeffer, M. Faibel, D. Nass, M. Hadani, Z. Ram, Convection-enhanced delivery of paclitaxel for the treatment of recurrent malignant glioma: a phase I/II clinical study, J. Neurosurg. 100 (2004) 472–479.
[16] S. Sugiyama, Y. Yamashita, T. Kikuchi, R. Saito, T. Kumabe, T. Tominaga, Safety and efficacy of convection-enhanced delivery of ACNU, a hydrophilic nitrosourea, in intracranial brain tumor models, J. Neurooncol. 82 (2007) 41–47.
[17] S. Sugiyama, Y. Yamashita, T. Kikuchi, Y. Sonoda, T. Kumabe, T. Tominaga, Enhanced antitumor effect of combined-modality treatment using convection-enhanced delivery of hydrophilic nitrosourea with irradiation or systemic administration of temozolomide in intracranial brain tumor xenografts, Neurol. Res. 30 (2008) 960–967.
[18] R. Saito, Y. Sonoda, T. Kumabe, K. Nagamatsu, M. Watanabe, T. Tominaga, Regression of recurrent glioblastoma infiltrating the brain stem after convection-enhanced delivery of nimustine hydrochloride, J. Neurosurg. Pediatr. 7 (2011) 522–526.
[19] K.S. Bankiewicz, J.L. Eberling, M. Kohutnicka, W. Jagust, P. Pivirotto, J. Bringas, J. Cunningham, T.F. Budinger, J. Harvey-White, Convection-enhanced delivery of AAV vector in parkinsonian monkeys; in vivo detection of gene expression and restoration of dopaminergic function using pro-drug approach, Exp. Neurol. 164 (2000) 2–14.
[20] R. Saito, J.R. Bringas, T.R. McKnight, M.F. Wendland, C. Mamot, D.C. Drummond, D.B. Kirpotin, J.W. Park, M.S. Berger, K.S. Bankiewicz, Distribution of liposomes into brain and rat brain tumor models by convection-enhanced delivery monitored with magnetic resonance imaging, Cancer Res. 64 (2004) 2572–2579.
[21] P.H. Chan, G.Y. Yang, S.F. Chen, E. Carlson, C.J. Epstein, Cold-induced brain edema and infarction are reduced in transgenic mice overexpressing CuZn-superoxide dismutase, Ann. Neurol. 29 (1991) 482–486.
[22] K. Murakami, T. Kondo, S. Sato, Y. Li, P.H. Chan, Occurrence of apoptosis following cold injury-induced brain edema in mice, Neuroscience 81 (1997) 231–237.
[23] R.D. Arnold, D.E. Mager, J.E. Slack, R.M. Straubinger, Effect of repetitive administration of doxorubicin-containing liposomes on plasma pharmacokinetics and drug biodistribution in a rat brain tumor model, Clin. Cancer Res. 11 (2005) 8856–8865.
[24] U.S. Sharma, A. Sharma, R.I. Chau, R.M. Straubinger, Liposome-mediated therapy of intracranial brain tumors in a rat model, Pharm. Res. 14 (1997) 992–998.
[25] C. Adamson, O.O. Kanu, A.I. Mehta, C. Di, N. Lin, A.K. Mattox, D.D. Bigner, Glioblastoma multiform: a review of where we have been and where we are going, Expert Opin. Invest. Drugs 18 (2009) 1061–1083.
[26] R. Saito, T. Kumabe, M. Kanamori, Y. Sonoda, T. Tominaga, Dissemination limits the survival of patients with anaplastic ependymoma after extensive surgical resection, meticulous follow up, and intensive treatment for recurrence, Neurosurg. Rev. 33 (2010) 185–191.
[27] M.M. Patel, B.R. Goyal, S.V. Bhadada, J.S. Bhatt, A.F. Amin, Getting into the brain: approaches to enhance brain drug delivery, CNS Drugs 23 (2009) 35–58.
[28] N.A. Vick, J.D. Khandekar, D.D. Bigner, Chemotherapy of brain tumors, Arch. Neurol. 34 (1977) 523–526.
[29] H. Nakagawa, D.R. Groothuis, E.S. Owens, J.D. Fenstermacher, C.S. Patlak, R.G. Blasberg, Dexamethasone effects on 125I-albumin distribution in experimental RG-2 gliomas and adjacent brain, J. Cereb. Blood Flow Metab. 7 (1987) 687–701.

J Neurosurg Pediatrics 7:522–526, 2011

Regression of recurrent glioblastoma infiltrating the brainstem after convection-enhanced delivery of nimustine hydrochloride

Case report

Ryuta Saito, M.D., Ph.D.,[1] Yukihiko Sonoda, M.D., Ph.D.,[1] Toshihiro Kumabe, M.D., Ph.D.,[1] Ken-ichi Nagamatsu, M.D., Ph.D.,[1] Mika Watanabe, M.D., Ph.D.,[2] and Teiji Tominaga, M.D., Ph.D.[1]

Departments of [1]Neurosurgery and [2]Pathology, Tohoku University Graduate School of Medicine, Sendai, Miyagi, Japan

This 13-year-old boy with a history of cranial irradiation for the CNS recurrence of acute lymphocytic leukemia developed a glioblastoma in the right cerebellum. Resection and chemo- and radiotherapy induced remission of the disease. However, recurrence was noted in the brainstem region 8 months later. Because no effective treatment was available for this recurrent lesion, the authors decided to use convection-enhanced delivery (CED) to infuse nimustine hydrochloride. On stereotactic insertion of the infusion cannula into the brainstem lesion, CED of nimustine hydrochloride was performed with real-time MR imaging to monitor the co-infused chelated gadolinium. The patient's preinfusion symptom of diplopia disappeared after treatment. Follow-up MR imaging revealed the response of the tumor. The authors report on a case of recurrent glioblastoma infiltrating the brainstem that regressed after CED of nimustine hydrochloride. *(DOI: 10.3171/2011.2.PEDS10407)*

Key Words • **convection-enhanced delivery** • **glioblastoma** • **brainstem** • **nimustine hydrochloride** • **gadolinium**

Gliomas diffusely affecting the brainstem have 2 different origins: one is the so-called brainstem glioma, and the other involves infiltration from gliomas originating in surrounding structures. Brainstem gliomas account for approximately 20% of all CNS tumors among children younger than 15 years of age. Among adults, brainstem gliomas are less common but have been reported in individuals up to the age of 70 years. Surgery no longer plays a role in diffuse brainstem glioma treatment. Meaningful resection is not possible, as the diffuse tumor is interwoven within white matter tracts traversing the brainstem, and resection does not confer a survival advantage.[4,14] Radiotherapy was previously the recommended treatment for all brainstem gliomas, leading to transient improvements in neurological function and a progression-free survival benefit, but it does not improve overall survival.[5] Currently, there is little, if any, evidence to suggest that chemotherapy has affected the outcome in patients with diffuse brainstem gliomas.[4,7] Consequently, the prognosis for diffuse brainstem glioma is very poor, with a median survival of less than 1 year. The median onset of disease progression following radiation is often less than 6 months, median survival is approximately 10 months, and less than 10% of patients are alive at 2 years.[5,6] Gliomas originating from surrounding structures such as the thalamus or cerebellum also infiltrate the brainstem, often at the time of recurrence. In this setting, it is more complicated because radiotherapy has already been administered in many cases at the time of initial therapy. Therefore, novel treatment modalities are required.

In the present report, we describe a case of recurrent glioblastoma affecting the brainstem that regressed after local ACNU-based chemotherapy. The local chemotherapy was administered using CED, aided by real-time MR imaging monitoring.[1–3,8,11,12]

Abbreviations used in this paper: ACNU = nimustine hydrochloride; CED = convection-enhanced delivery; Gd-DOTA = gadoterate meglumine.

Case Report

History. This 13-year-old boy developed truncal and right cerebellar ataxia, and he visited the department of pediatrics at our hospital in October 2008. He had a history of acute lymphocytic leukemia (French-American-British Class L1) and underwent chemotherapy at the age of 2 years. Recurrent disease in his testis and CNS was detected when he was 5 and 8 years of age, respectively. Both recurrent lesions were treated with combined chemo- and radiotherapy including 18-Gy whole-brain and whole-spine irradiation at 8 years of age. After these treatments, complete remission of the acute lymphocytic leukemia was achieved without any systemic or neurological deficits. However, in October 2008, T2-weighted MR imaging of the brain revealed a massive high-intensity lesion in the right cerebellar hemisphere (Fig. 1A). Contrast-enhanced T1-weighted MR imaging revealed spotty enhancement within the lesion (Fig. 1B). Magnetic resonance spectroscopy detected an elevated choline peak in the lesion. With a diagnosis of malignant glioma, he was referred to our department.

Treatment. The tumor was subtotally resected in November 2008 (Fig. 1C and D). After surgery, the patient underwent local radiotherapy (50 Gy) and concomitant temozolomide therapy. Exhibiting just slight ataxia, he was discharged from the hospital to home and enjoyed his school life until May 2009 (Fig. 1E and F). During this period, temozolomide-based chemotherapy was continued on an outpatient basis. On follow-up outpatient MR imaging in June 2009, slight enhancement was noted in the brainstem (Fig. 2A). Considering a differential diagnosis of tumor recurrence and radiation necrosis, we conducted further examinations. A methionine-based PET study revealed a high uptake (maximal standardized uptake value = 4.2) (Fig. 2B), suggesting a tumor recurrence, and MR images obtained simultaneously depicted the enlargement of the enhanced tumor (Fig. 2C). At this point, we decided to perform CED of ACNU. During the preparation period of only 16 days, we observed additional enlargement of the enhanced tumor (Fig. 2D). The patient developed diplopia due to right-side medial-longitudinal-fasciculus syndrome. After planning the route for the catheter (iPlan stereotactic software, Brainlab), an 18-gauge 30-cm single-lumen central venous catheter (UNITIKA) was inserted via the left frontal lobe with stereotactic assistance (Fig. 3A–C). Nimustine hydrochloride solution, which contained 0.25 mg/ml of ACNU and 1 mM Gd-DOTA in saline, was infused over 2.5 days through the inserted catheter, using the CED method. Briefly, using a microinfusion pump, the infusion rate was controlled and gradually increased from 1.0 to 5.0 μl/min, resulting in a total infusion of 7020 μl after 2.5 days. Oral temozolomide at 200 mg/m^2/day was used simultaneously for 5 sequential days starting from the day of catheter insertion. Intravenous dexamethasone was also used during infusion. Magnetic resonance images were obtained during and after infusion. Noncontrast T1-weighted MR imaging revealed the delivery of Gd-DOTA that was mixed in the infusion solution (Fig. 3D–G). The volume of distribution was plotted against the volume of infusion (Fig. 3H). We calculated the volume of distribution as the volume of distribution from MR images containing at least 10% of the total increase in signal intensity due to the addition of contrast agent as reported previously.[13] The images in Fig. 4 (A–D) demonstrate the relationship of the tumor and distribution of Gd-DOTA at the end of

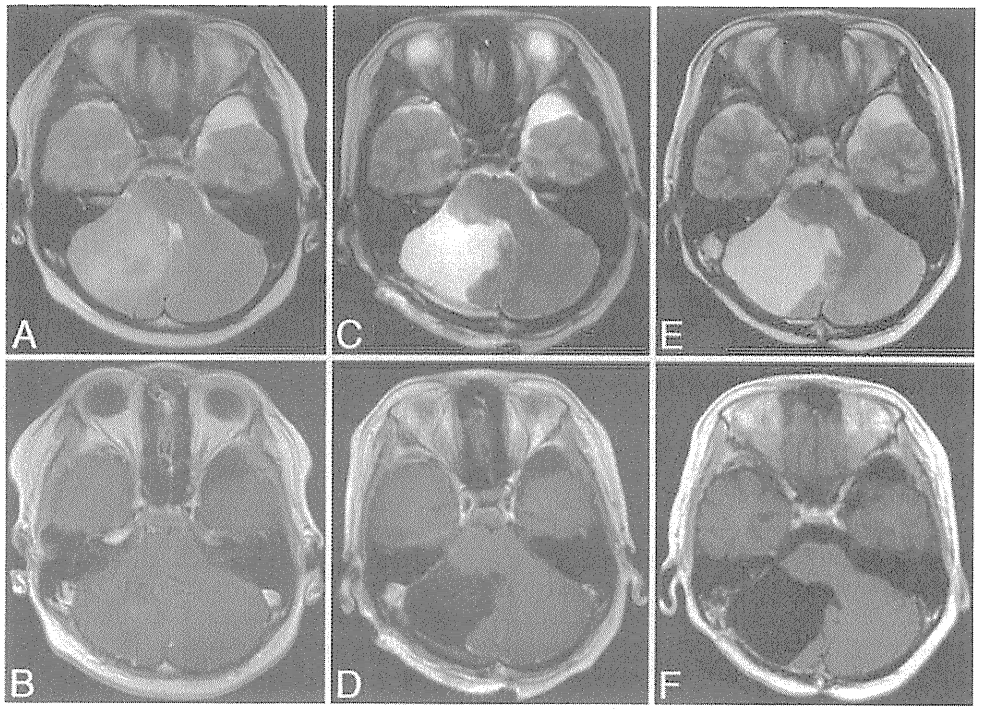

FIG. 1. Axial T2-weighted (**A, C, and E**) and contrast-enhanced T1-weighted (**B, D, and F**) MR images obtained at diagnosis in October 2008 (**A and B**), after tumor resection (**C and D**), and at follow-up in May 2009 (**E and F**).

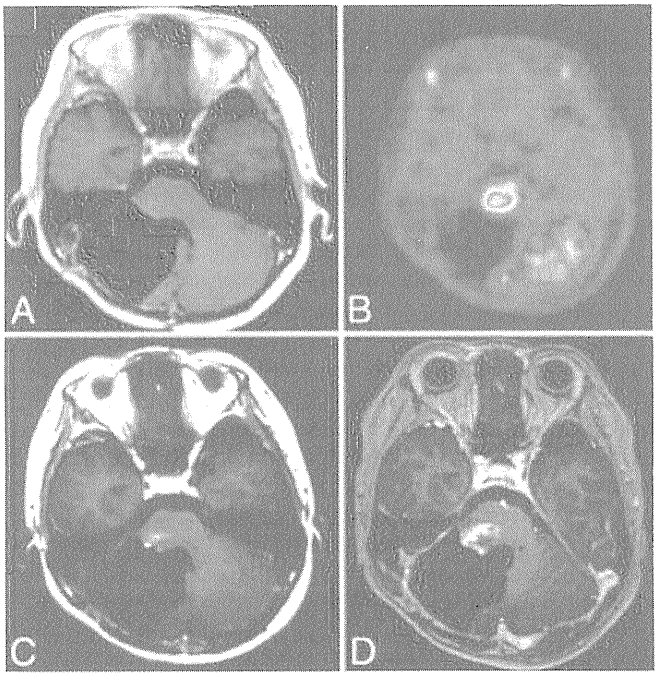

FIG. 2. Axial contrast-enhanced T1-weighted MR images obtained in June 2009 when recurrence in the brainstem was suspected (A), 6 days later (C) obtained together with a methionine-based PET scan (B), and 16 days later just before treatment CED (D).

CED. During the infusion, when infusion reached 2000 μl, slight aggravation of right-side medial-longitudinal-fasciculus syndrome was observed. Development of mild right hemiparesis was noted 4 days after the termination of infusion, which fully recovered within a week. On a diffusion-weighted MR image obtained when hemiparesis was recognized, we noted a spotty high-intensity lesion in the left corona radiata (Fig. 4E). As Gd-DOTA was also found at this site in the image obtained at the end of infusion (Fig. 4F), we considered this to represent a side effect of the delivered ACNU. Otherwise, the clinical course after CED was uneventful. The diplopia and right hemiparesis resolved. The patient returned to normal school life with the continuation of monthly temozolomide. Contrast-enhanced T1-weighted MR imaging revealed the shrinkage of the brainstem lesion (Fig. 5). Unfortunately in December 2009, the patient was readmitted to our hospital with the rapid progression of multiple disseminated diseases. In late January 2010, he died.

Discussion

We have been working toward the CED of ACNU to treat malignant gliomas. In our first article published in 2007, we demonstrated the efficacy of ACNU in a rodent intracranial xenograft tumor model.[18] The subsequent publication demonstrated the efficacy of combination therapy using CED of ACNU and systemic temozolomide.[19] We then concluded a toxicity study in nonhuman primates (unpublished data). Histological examination revealed minimum tissue damage after a 1-mg/ml infusion of ACNU, which was the safety dose detected in our previous rodent study. Based on these results, we started a pilot clinical study in 2008 on the CED of ACNU in patients with recurrent high-grade glioma after being granted approval from our institutional ethical committee. To treat recurrent high-grade gliomas, we used a mixture of ACNU and Gd-DOTA in CED. Starting from the day of infusion, temozolomide was also given orally for 5 consecutive days according to the protocol for recurrent disease. The present case was a patient involved in the study.

The treatment of a recurrent glioma affecting the brainstem is challenging. No effective therapy is available for patients in whom chemo- and radiotherapy have already been given for the initial disease. In the present case, the rapid progression of recurrent disease was detected on

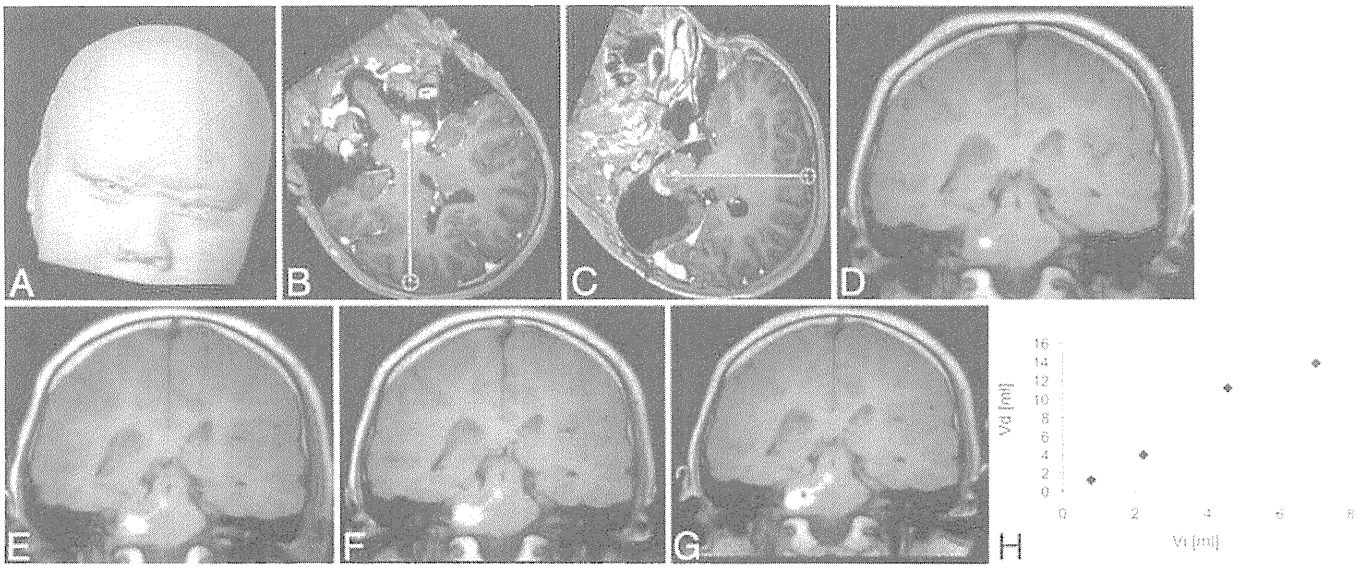

FIG. 3. A–C: Route of the catheter tract developed. D–G: Coronal T1-weighted MR images obtained during the CED of ACNU. The images were acquired when the infusion volumes were 780, 2220, 4560, and 7020 μl, respectively. H: Volume of distribution (Vd) was plotted against volume of infusion (Vi) at 4 different time points.

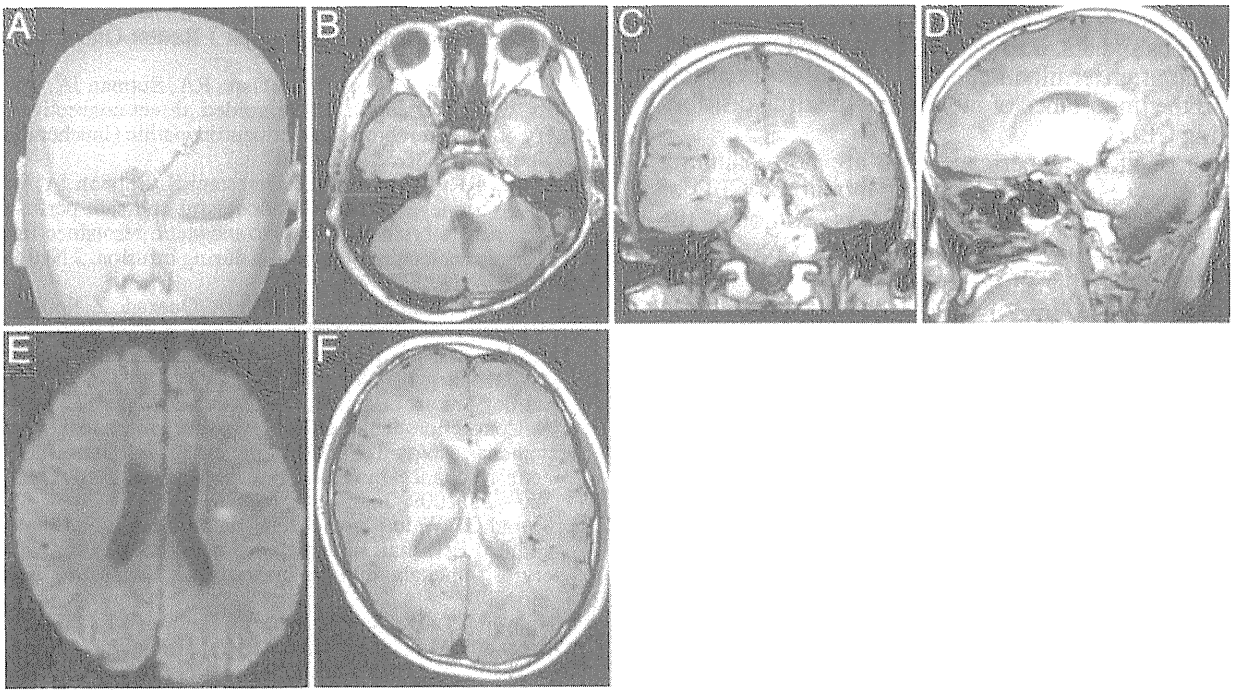

FIG. 4. Relationship between the enhanced tumor mass and distribution of CED Gd-DOTA. **A–D and F:** Images produced using the iPlan stereotactic software. The contrast-enhanced T1-weighted MR image are overlapped with the T1-weighted MR images obtained at the end of CED. The tumor is indicated by the *red* and the distribution of Gd-DOTA by *yellow*. The images in **A–D** demonstrate the relationship between the tumor and distribution of Gd-DOTA at the end of CED. Diffusion-weighted MR images, obtained when the patient developed mild right hemiparesis (**E**), showing a high-intensity lesion in the left corona radiata where there was a reflux of infused Gd-DOTA at the end of infusion (**F**).

MR imaging together with the rapid deterioration of diplopia. Methionine-based PET scanning detected a region of high uptake corresponding to the brainstem lesion, which suggested "recurrence" rather than radiation necrosis. We observed that CED of ACNU demonstrated the efficacy against this lesion. Regression of the lesion was documented together with the disappearance of diplopia. Although dissemination developed 5 months after CED, our patient was able to resume his school life until then. An important motivation for the development of CED has been the desire to offer a new treatment to children with diffuse pontine gliomas.[9,10,17,20,21] In the present case the patient did not have diffuse pontine glioma, but the condition treated is similar. Thus, results in this case indicate a promise for future development of this delivery strategy.

Visualization of drug distribution during CED is also of importance in the future development of CED.[8–13,15,16] The Gd-DOTA used in this study provided important information on drug delivery. Although it is not clear if the Gd-DOTA distribution directly reflects that of ACNU, there were findings that suggested a similarity in the distribution. Magnetic resonance imaging detected the backflow of Gd-DOTA through the catheter tract. The backflow was detected at the catheter tract penetrating the corona radiata of the left hemisphere. During infusion, we were anxious about this because, if the distribution of ACNU was the same as that of Gd-DOTA, this might cause some damage to the left corona radiata. Actually, the patient developed mild right hemiparesis after infusion. On diffusion-weighted MR imaging, performed when hemiparesis was

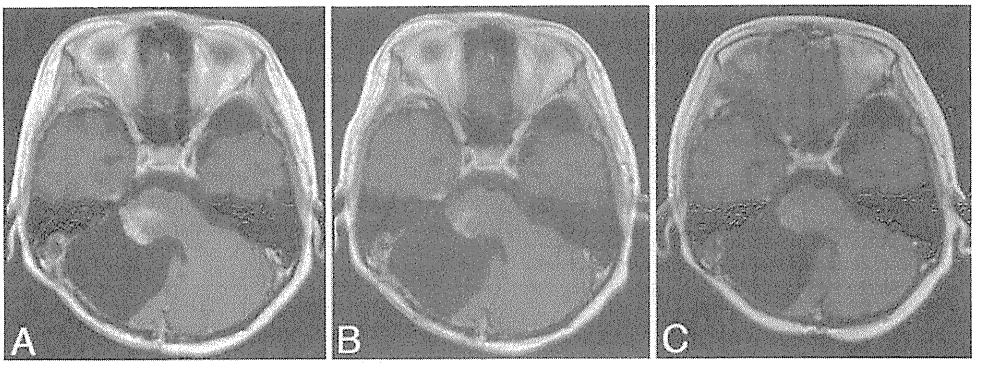

FIG. 5. Axial contrast–enhanced T1-weighted MR images obtained 1 week after CED (**A**), 1 month after CED (**B**), and 3 months after CED (**C**).

recognized, we observed a spotty high-intensity lesion in the left corona radiata. Fortunately, this symptom fully resolved soon after termination of the CED. However, this suggested the importance of monitoring the drug distribution during CED.

Based on these experiences, we are now planning a Phase I study on the MR imaging–monitored CED of ACNU for recurrent brainstem gliomas. Although the treatment of this disease is challenging, the present case suggests the possibility of using CED against this devastating disease. We can only treat localized disease with CED, and we still need to develop an effective treatment against disseminated disease. However, localized disease should be cured beforehand. Together with imaging guidance, this platform of therapy may provide an alternative therapeutic strategy to brainstem gliomas in the future.[13,15]

Conclusions

The present case of recurrent glioblastoma affecting the brainstem suggests the efficacy of local chemotherapy aided by CED. Regression of the enhanced tumor as well as symptoms was achieved even with the recurrent, rapidly progressing disease. Although the patient finally died of disseminated disease, the CED of ACNU facilitated local control of the disease even in the brainstem region. Based on these experiences, we are now preparing a Phase I study on the MR imaging–monitored CED of ACNU for recurrent brainstem gliomas.

Disclosure

The authors report no conflict of interest concerning the materials or methods used in this study or the findings specified in this paper.

Author contributions to the study and manuscript preparation include the following. Author contributions to the study and manuscript preparation include the following. Conception and design: Saito. Acquisition of data: Saito, Sonoda, Kumabe, Nagamatsu, Watanabe. Analysis and interpretation of data: Saito, Sonoda, Kumabe, Nagamatsu. Drafting the article: Saito. Critically revising the article: Sonoda, Kumabe, Watanabe. Reviewed final version of the manuscript and approved it for submission: all authors. Study supervision: Tominaga.

References

1. Degen JW, Walbridge S, Vortmeyer AO, Oldfield EH, Lonser RR: Safety and efficacy of convection-enhanced delivery of gemcitabine or carboplatin in a malignant glioma model in rats. **J Neurosurg 99:**893–898, 2003
2. Ding D, Kanaly CW, Bigner DD, Cummings TJ, Herndon JE II, Pastan I, et al: Convection-enhanced delivery of free gadolinium with the recombinant immunotoxin MR1-1. **J Neurooncol 98:**1–7, 2010 (Erratum in **J Neurooncol 98:**9, 2010)
3. Ding D, Kanaly CW, Cummings TJ, Ii JE, Raghavan R, Sampson JH: Long-term safety of combined intracerebral delivery of free gadolinium and targeted chemotherapeutic agent PRX321. **Neurol Res** [epub ahead of print], 2009
4. Donaldson SS, Laningham F, Fisher PG: Advances toward an understanding of brainstem gliomas. **J Clin Oncol 24:**1266–1272, 2006
5. Frazier JL, Lee J, Thomale UW, Noggle JC, Cohen KJ, Jallo GI: Treatment of diffuse intrinsic brainstem gliomas: failed approaches and future strategies. A review. **J Neurosurg Pediatr 3:**259–269, 2009
6. Freeman CR, Farmer JP: Pediatric brain stem gliomas: a review. **Int J Radiat Oncol Biol Phys 40:**265–271, 1998
7. Jalali R, Raut N, Arora B, Gupta T, Dutta D, Munshi A, et al: Prospective evaluation of radiotherapy with concurrent and adjuvant temozolomide in children with newly diagnosed diffuse intrinsic pontine glioma. **Int J Radiat Oncol Biol Phys 77:**113–118, 2010
8. Lonser RR, Schiffman R, Robison RA, Butman JA, Quezado Z, Walker ML, et al: Image-guided, direct convective delivery of glucocerebrosidase for neuronopathic Gaucher disease. **Neurology 68:**254–261, 2007
9. Lonser RR, Walbridge S, Garmestani K, Butman JA, Walters HA, Vortmeyer AO, et al: Successful and safe perfusion of the primate brainstem: in vivo magnetic resonance imaging of macromolecular distribution during infusion. **J Neurosurg 97:**905–913, 2002
10. Lonser RR, Warren KE, Butman JA, Quezado Z, Robison RA, Walbridge S, et al: Real-time image-guided direct convective perfusion of intrinsic brainstem lesions. Technical note. **J Neurosurg 107:**190–197, 2007
11. Mardor Y, Last D, Daniels D, Shneor R, Maier SE, Nass D, et al: Convection-enhanced drug delivery of interleukin-4 Pseudomonas exotoxin (PRX321): increased distribution and magnetic resonance monitoring. **J Pharmacol Exp Ther 330:**520–525, 2009
12. Murad GJ, Walbridge S, Morrison PF, Szerlip N, Butman JA, Oldfield EH, et al: Image-guided convection-enhanced delivery of gemcitabine to the brainstem. **J Neurosurg 106:**351–356, 2007
13. Nguyen TT, Pannu YS, Sung C, Dedrick RL, Walbridge S, Brechbiel MW, et al: Convective distribution of macromolecules in the primate brain demonstrated using computerized tomography and magnetic resonance imaging. **J Neurosurg 98:**584–590, 2003
14. Pierre-Kahn A, Hirsch JF, Vinchon M, Payan C, Sainte-Rose C, Renier D, et al: Surgical management of brain-stem tumors in children: results and statistical analysis of 75 cases. **J Neurosurg 79:**845–852, 1993
15. Saito R, Bringas JR, McKnight TR, Wendland MF, Mamot C, Drummond DC, et al: Distribution of liposomes into brain and rat brain tumor models by convection-enhanced delivery monitored with magnetic resonance imaging. **Cancer Res 64:**2572–2579, 2004
16. Saito R, Krauze MT, Bringas JR, Noble C, McKnight TR, Jackson P, et al: Gadolinium-loaded liposomes allow for real-time magnetic resonance imaging of convection-enhanced delivery in the primate brain. **Exp Neurol 196:**381–389, 2005
17. Sandberg DI, Edgar MA, Souweidane MM: Convection-enhanced delivery into the rat brainstem. **J Neurosurg 96:**885–891, 2002
18. Sugiyama S, Yamashita Y, Kikuchi T, Saito R, Kumabe T, Tominaga T: Safety and efficacy of convection-enhanced delivery of ACNU, a hydrophilic nitrosourea, in intracranial brain tumor models. **J Neurooncol 82:**41–47, 2007
19. Sugiyama S, Yamashita Y, Kikuchi T, Sonoda Y, Kumabe T, Tominaga T: Enhanced antitumor effect of combined-modality treatment using convection-enhanced delivery of hydrophilic nitrosourea with irradiation or systemic administration of temozolomide in intracranial brain tumor xenografts. **Neurol Res 30:**960–967, 2008
20. Thomale UW, Tyler B, Renard VM, Dorfman B, Guarnieri M, Haberl HE, et al: Local chemotherapy in the rat brainstem with multiple catheters: a feasibility study. **Childs Nerv Syst 25:**21–28, 2009
21. Yin D, Richardson RM, Fiandaca MS, Bringas J, Forsayeth J, Berger MS, et al: Cannula placement for effective convection-enhanced delivery in the nonhuman primate thalamus and brainstem: implications for clinical delivery of therapeutics. Laboratory investigation. **J Neurosurg 113:**240–248, 2010

Manuscript submitted September 8, 2010.
Accepted February 11, 2011.

Address correspondence to: Ryuta Saito, M.D., Ph.D., Department of Neurosurgery, Tohoku University Graduate School of Medicine, 1-1 Seiryo-machi, Aoba-ku, Sendai, 980-8574, Japan. email: ryuta@nsg.med.tohoku.ac.jp.

J Neurooncol (2011) 104:779–787
DOI 10.1007/s11060-011-0544-2

CLINICAL STUDY – PATIENT STUDY

Logarithmic decrease of serum alpha-fetoprotein or human chorionic gonadotropin in response to chemotherapy can distinguish a subgroup with better prognosis among highly malignant intracranial non-germinomatous germ cell tumors

Tomohiro Kawaguchi · Toshihiro Kumabe · Masayuki Kanamori · Ryuta Saito · Yoji Yamashita · Yukihiko Sonoda · Mika Watanabe · Teiji Tominaga

Received: 16 August 2010 / Accepted: 15 February 2011 / Published online: 26 February 2011

Abstract Intracranial non-germinomatous germ cell tumors (NGGCTs) are a heterogeneous group of tumors. Although alpha-fetoprotein (AFP) and human chorionic gonadotropin (HCG) are considered reliable markers for making diagnosis, the relationship between serum concentration of them and prognosis remains unclear. The present study investigated the decrease of serum tumor markers AFP and HCG as prognostic factors for patients with highly malignant NGGCTs. Eight consecutive patients with AFP > 1000 ng/ml or HCG > 2000 mIU/ml at initial treatments after January 2004 were retrospectively reviewed. Serum AFP or HCG concentration and tumor volume were sequentially measured during the therapeutic period. Six patients were treated by neoadjuvant chemotherapy consisting of ifosfamide, cisplatin, and etoposide, followed by salvage surgery and/or radiation therapy. A 14-year-old boy with choriocarcinoma and a 2-year-old boy with yolk sac tumor underwent radical resection because of acute hydrocephalus and mass effect on the brain stem, followed by chemotherapy and radiation therapy. Five patients showed complete response and survived at follow-up periods of 9, 26, 41, 63, and 75 months, and the other three showed partial response but subsequent recurrence, finally died. Patients with complete response showed logarithmic decrease of serum AFP to the normal range in response to chemotherapy, but the others did not. Logarithmic decrease and normalization of serum AFP and HCG levels during neoadjuvant chemotherapy can distinguish a subgroup with better prognosis within highly malignant NGGCTs. To determine it, sequential measurement of serum tumor marker level was efficient. Outcomes were still dismal for slow responding patients, but this simple method may indicate more aggressive therapy.

Keywords Non-germinomatous germ cell tumors · Neoadjuvant chemotherapy · Alpha-fetoprotein · Human chorionic gonadotropin · Outcome

T. Kawaguchi · T. Kumabe (✉) · M. Kanamori · R. Saito · Y. Yamashita · Y. Sonoda · T. Tominaga
Department of Neurosurgery, Tohoku University Graduate School of Medicine, 1-1 Seiryo-machi, Aoba-ku, Sendai, Miyagi 980-8574, Japan
e-mail: kuma@nsg.med.tohoku.ac.jp

M. Watanabe
Department of Pathology, Tohoku University Hospital, Sendai, Miyagi, Japan

Introduction

Intracranial germ cell tumors consist of a heterogeneous group of tumors including pure germinoma, mature and immature teratomas, teratomas with malignant transformation, yolk sac tumors, choriocarcinomas, embryonal carcinomas, and mixed tumors, which account for 2.8% of all primary brain tumors in Japan [1]. The histological subtype is the single most predictive factor of outcomes [2], as germinomas are curable using only radiation therapy with 10-year overall survival rates >90% [3, 4], whereas non-germinomatous germ cell tumors (NGGCTs) are relatively resistant to radiation therapy and chemotherapy with poor outcomes [5–8]. NGGCTs can be divided into three groups: mature teratoma forms the good prognosis group; immature teratoma, teratoma with malignant transformation, and mixed tumors mainly consisting of germinomas or teratomas form the intermediate group; and yolk sac tumor, embryonal carcinoma, choriocarcinoma, and mixed tumors consisting mainly of these histological subtypes form the poor prognosis group [9].

Neoadjuvant chemotherapy has dramatically improved the clinical outcome [10, 11]. The Japanese Pediatric Brain Tumor Study Group (JPBTSG) conducted a multiinstitutional Phase II trial to investigate the efficacy of platinum-based chemotherapy combined with radiation therapy [7, 9]. Patients were treated with only chemotherapy, followed by radiation therapy after surgical debulking of the tumor to obtain the histological verification. The protocol was effective for patients in the good or intermediate prognosis groups, but in patients in the poor prognosis group showed rapid tumor progression and could not be rescued. Therefore, tumors in the poor prognosis group require combined systemic chemotherapy and whole craniospinal radiation therapy to achieve better outcomes. On the other hand, severe complications such as prolonged myelosuppression due to the combined intensive treatment cannot be denied, so it remains unclear when to start such an intensive treatment.

Recently, the 2- and 5-year survival rates of patients with choriocarcinoma were reported as 49.8% [12], indicating that half of the patients died in the early therapeutic stage and the other half survived longer than expected. Our recent study showed the same tendency in patients with NGGCT in the poor prognosis group [6]. These observations led us to the idea that patients with poor prognosis NGGCT can be divided into two subgroups: responders to neoadjuvant chemotherapy with better prognosis and non-responders or treatment relapse with extremely poor prognosis. Discrimination of these subgroups should lead to optimum treatment efforts.

Alpha-fetoprotein (AFP) and human chorionic gonadotropin (HCG) are the most reliable tumor markers to define the histological subtype of NGGCT. AFP is normally produced by the fetal yolk sac and other organs, and is essentially undetectable in the serum in normal adults. High serum AFP concentrations are mainly found in patients with yolk sac tumor, and less often in patients with embryonal carcinoma, except for hepatocellular carcinoma. HCG, especially the beta subunit of HCG, is produced by NGGCTs that consist of pure or mixed embryonal carcinoma or choriocarcinoma. These tumor markers have clear roles in the diagnosis, staging, risk classification, and clinical management of testicular germ cell tumors [13–15]. The SIOP CNS-GCT-96 (International Society of Paediatric Oncology Central Nervous System-Germ Cell Tumor-1996) protocol reported AFP > 1000 ng/ml at diagnosis and/or residual disease after treatment were risk factors for relapse of NGGCTs [16], but the relationship between serum tumor marker concentration and prognosis remains unclear in patients with intracranial germ cell tumor.

The present study retrospectively analyzed the treatment outcome of patients with intracranial NGGCT in the poor prognosis group, most of them were treated with neoadjuvant chemotherapy. The study suggests that sequential decrease of serum tumor marker concentration may provide an additional prognostic factor for patients with highly malignant NGGCTs and be useful to determine when to start more aggressive treatment.

Clinical materials and methods

This study included eight consecutive patients with NGGCT with elevated serum AFP (>1000 ng/ml) or HCG (>2000 mIU/ml) level treated with chemotherapy, radiation therapy, or surgery at Tohoku University Hospital since January 2004. Some of these patients were described previously [6, 17, 18]. We reviewed the clinical history, radiographical findings, treatment, and histological findings. The serum concentrations of the tumor markers were analyzed on admission before beginning treatment and were sequentially followed during the treatment period. In addition, concentrations of the tumor markers in cerebrospinal fluid (CSF) were also analyzed in some patients. Tumor location and volume were sequentially evaluated by magnetic resonance (MR) imaging with contrast medium. Volumetric analysis was performed using OsiriX imaging software version 2.7.5 (The OsiriX Foundation, Geneva, Switzerland). The diagnosis of NGGCT was based on the clinical findings, radiographical findings, tumor location, and/or histological verification based on the World Health Organization classification [2, 6].

The therapy protocol was based on the JPBTSG recommendations. Patients received 3 cycles of chemotherapy (ICE regimen) using ifosfamide (900 mg/m^2 on Days 1–5), cisplatin (20 mg/m^2 on Days 1–5), and etoposide (60 mg/m^2 on Days 1–5) at 4-week intervals, followed by radiation therapy to the whole craniospinal axis and the extended local field. Salvage surgery was performed after or during chemotherapy and radiation therapy if complete remission was not achieved. Thereafter, 1–5 cycles of maintenance chemotherapy was carried out as well.

The normal levels of the serum AFP and HCG concentration in our institute are <20 ng/ml and <1 mIU/ml, respectively. The sequential serum concentrations of AFP and HCG were plotted on time series graphs and compared to the ideal decrement rates, those are theoretical values based on biological serum half lives of those tumor markers. Informed consent was obtained from all patients or their guardians involved in this study.

Results

Patient characteristics are summarized in Table 1. Six of eight patients showed elevated serum AFP levels and the others showed elevated serum HCG levels.

Table 1 Characteristics of eight patients with non-germinomatous germ cell tumor

	Age (years)/ sex	Location	Pretreatment		Nadir after treatment		Radiographical response to initial chemotherapy	Additional treatment	Surgery	Local recurrence	Dissemination	Outcome	Histology	OS (months)	PFS (months)
			Serum AFP (ng/ml)	Serum HCG (mIU/ml)	Serum AFP (ng/ml)	Serum HCG (mIU/ml)									
1	2/M	V	7094	WNL	22.2	WNL	No target lesion	Chemo + Rad + GKS	GTR	None	Yes	PD → D	YST	23 D	6
2	7/M	BG	1321	98.2	WNL	WNL	PR	Chemo + Rad	GTR	None	None	CR	MT	63A	63
3	14/M	P	WNL	16632	WNL	1	No target lesion	Chemo + Rad	GTR	None	None	CR	CC	41A	41
4	15/M	P	5235	WNL	WNL	WNL	PR	Rad[b]	GTR	None	None	CR	MT	9 A	9
5	15/M	BG	4941	WNL	35.1	WNL	PD	Chemo + Rad + GKS	STR	Yes	Yes	PD → D	YST	17 D	3
6	18/M	T	WNL	9359	WNL	1	PR	Chemo + Rad	GTR	None	None	CR	Necrosis and CC	26 A	26
7	22/F	S/P	651.6[a]	WNL	WNL	WNL	PR	Chemo + Rad	None	None	None	CR	None	75 A	75
8	34/M	P	2909	WNL	422.9	WNL	PR	Chemo + Rad + GKS	None	None	Yes	PD → D	YST[c]	9 D	4

A alive, *AFP* alpha-fetoprotein, *BG* basal ganglia, *CC* choriocarcinoma, *Chemo* chemotherapy, *CR* complete response, *D* dead, *F* female, *GKS* gamma knife surgery, *GTR* gross total resection, *HCG* human chorionic gonadotropin, *M* male, *MT* mature teratoma, *OS* overall survival, *P* pineal region, *PD* progression disease, *PFS* progression free survival, *PR* partial response, *Rad* radiation, *S* suprasellar region, *STR* subtotal resection, *T* thalamus, *V* vermis, *WNL* within normal limits, *YST* yolk sac tumor

[a] Serum AFP concentration was 651.6 ng/ml on admission, but rose to 1765.8 ng/ml 10 days after chemotherapy induction

[b] Maintenance chemotherapy has been planned

[c] The histological examination had been done by autopsy